Murine cytomegalovirus promotes renal allograft inflammation via Th1/17 cells and IL-17A.

Ravi Dhital, Shashi Anand, Brianna Graber, Qiang Zeng, Victoria M. Velazquez, Srinivasa R. Boddeda, James R. Fitch, Ranjana W. Minz, Mukut Minz, Ashish Sharma, Rachel Cianciolo and Masako Shimamura

SUPPLEMENTAL DATA

SUPPLEMENTAL MATERIAL AND METHODS

S.1. MCMV lysate and peptide pool comparison for T cell stimulation

MCMV lysates were prepared by high-speed centrifugation method. In brief, MCMVΔm157 infected, p53 deficient (p53-/-) mouse embryogenic fibroblasts (gift of W. Britt, University of Alabama at Birmingham, Birmingham AL) were lysed by 2 cycles of freeze-thaw and cellular debris pelleted by low-speed centrifugation at 2000 x g (Sorvall Legend XTR, Thermo Scientific) for 10 minutes at 4°C. Supernatants were subjected to high-speed centrifugation at 16,000 x g for 2 hours at 4°C (Sorvall LYNX 6000, Thermo Scientific). The virus pellet was suspended in 0.9% NaCl and sonicated on ice at 20kHz frequency and 70% amplitude for 15 seconds x 3 cycles (FB505, Fisher Scientific). The protein content of the viral lysate was quantified using BCA protein assay kit (Thermo Scientific, Waltham, MA), aliquoted and stored at -80°C.

Splenocytes from D+R+ transplants were stimulated with 5 µg/ml of either MCMV lysate or a pool of 15 class II-restricted MCMV peptides (Table S1), stained for IFN-γ, TNF-α and IL-17A, and frequencies of CD4$^+$ T cells expressing cytokines calculated after lysate or peptide stimulation. Peptide stimulation yielded similar or higher frequencies of cytokine-expressing MCMV-specific CD4 T cells compared to viral lysate stimulation (Figure S2), so peptide antigen stimulation was utilized for all transplant studies.

S.2. Intracellular cytokine staining by flow cytometry.

Cells were either unstimulated or stimulated with either PMA or MCMV peptide pool for 6 hours in presence of brefeldin A, blocked with anti-CD16/32, stained for surface markers and viability (Table S2), fixed, permeabilized and stained for intracellular cytokines (ICS) and transcription factors. Isotype matched antibodies and MHC-I-A^b huCLIP were used as staining controls. Stained

cells were acquired in a LSRII Fortessa or Attune NxT cytometers and analyzed using FlowJo V10 software. APC labelled I-A^b-AAHAEINEA$_{329-337}$ (chicken ovalbumin) and I-A^b-PVSKMRMATPLLMQA$_{87-101}$ (human CLIP) tetramers were synthesized by the NIH tetramer Core Facility**.**

S.3. RNA-Seq analysis

Total RNA from D+ and D- allografts or kidneys of MCMV infected- and uninfected- BALB/c mice was isolated and purified using the RNeasy Mini Kit and RNeasy MinElute Cleanup kit (Qiagen, Germantown MD) according to the manufacturer's instructions, and purified RNA was treated with DNase (Qiagen) to remove DNA. RNA purity was confirmed using a Nanodrop spectrophotometer (Thermo Fisher, Waltham MA). RNA integrity was assessed using Eukaryote Total RNA Nano Kit on the Bioanalyzer 2100 system (Agilent Technologies, Santa Clara CA). 500 ng of RNA, per sample, was used as input for RNA library preparation. Libraries were generated using the Total RNA TruSeq kit (Illumina, San Diego CA) with Ribo-Zero Complete Globin kit (Illumina) following manufacturer's recommendations and indices were added to multiplex the data. Final library quality was assessed using the High Sensitivity D1000 kit on the 4200 Tapestation (Agilent). Paired end 150 base pair sequencing was performed on the HiSeq 4000 (Illumina). Each sample was aligned to the GRCm38.p4 assembly of the mouse reference from NCBI using version 2.6.0c of the RNA-Seq aligner STAR.[1] Transcript features were identified from the GFF file provided with the assembly from NCBI and raw coverage counts were calculated using HTSeq. The raw RNA-Seq gene expression data was normalized and post-alignment statistical analyses were performed using DESeq2[2] and custom analysis scripts written in R. Comparisons of gene expression and associated statistical analysis were made between different conditions of interest using the normalized read counts. All fold change values are expressed as test condition/control condition, where values less than 1 are denoted as the negative of its inverse. Transcripts were considered significantly differentially expressed using a 10% false discovery rate (DESeq2 adjusted p value <= 0.1). The QIAGEN Ingenuity Pathway Analysis software (Qiagen Science, Germantown, MD) was used for canonical pathway analysis and differential gene expression.

S.4. MCMV viral load quantitation

Viral DNA was extracted from tissues using the Zymo viral DNA (Quick-DNA Viral Kit, Zymo Research, Irvine, CA). Quantitative DNA PCR was performed using primers and probes for MCMV immediate- early 1 (IE1) exon 4 (Table S4) in comparison with a standard curve generated by a plasmid encoding the IE1 exon 4 sequence.[3] The PCR reaction was performed using TaqMan Gene Expression Master Mix and a StepOnePlus Real- Time PCR system (Applied Biosystems, Foster City, CA) with amplification conditions of 50°C for 5 minutes, followed by 95°C for 10 min, 40 cycles of 95° for 0.15 seconds and 64°C for 1 min, and a final step of 72°C for 5 min. Viral loads in plasma were expressed as copies/ml whereas, viral loads in tissue were expressed as copies/ g of tissue.

S.5. *In vivo* IL-17A neutralization and Tregs depletion

Kidney transplant recipients were injected intraperitoneally with 200 µg of rat-anti-mouse IL-17A (Clone 17F3, BioXCell, West Lebanon, NH) or isotype matched control antibodies at post-transplant days 1, 3, 5, 7, 9, 12 until terminal sacrifice. Rat-anti-mouse CD25 (clone PC61, Leinco Technologies, St. Louis, MO) or isotype control antibodies were injected intraperitoneally on days 1 (400 µg) and 4 (200 µg) post-transplant to deplete regulatory T-cells (Tregs). The effectiveness of Treg depletion by αCD25 antibodies was first tested in non-transplant mice, with depletion of ~60-80% of Foxp3+ Tregs confirmed at days 4 (one dose) and 7 (2 doses) post treatment.

S.6. Human renal transplant cohort study

A retrospective cohort study was conducted at PGIMER to investigate the genetic, phenotypic and functional variations of T and B cells at the time of renal allograft rejection.[4-6] For the parent study, adults (age >18 years) diagnosed with end stage renal disease undergoing first renal transplantation between July 2012 and August 2013 were included in the study after obtaining their written informed consent. Exclusion criteria were recipients of multiorgan or prior organ transplant and known HIV, hepatitis B or C infection. The recipients were followed for 12 months post-transplant. Demographic and clinical data were collected: donor and recipient age and sex, recipient's disease history, HLA types, cross match, induction immunosuppression, graft ischemia time, post-transplant creatinine and immunosuppressant levels. For rejection episodes, histopathologic rejection classification and DSA status were collected from the clinical record. Blood was collected from all subjects at pre-transplant, 1-, 3-, 6- and 12-months post-transplant

and at the time of rejection. For this study, a retrospective cohort study was performed to determine the association between blood mRNA RORγt: FOXP3 ratio and acute renal allograft rejection. The study was approved as exempt research under the category of secondary research using previously collected specimen by the PGIMER institutional review board (Endorsement No. 8766-PG-10-1TRG/8448). Cases of acute allograft rejection (AR) were identified by searching the database. Eligible cases included all the recipients with acute cell mediated allograft rejection (N= 18) and acute mixed allograft rejection (N=6). A control cohort of 29 recipients without acute rejection were matched with the cases for age and sex. AR cases with cell mediated or mixed rejection were matched by age and sex with controls without AR. Blood RNA was analyzed by RT-PCR for *RORγt, FOXP3* and *β-actin* expression (Supplemental Methods S.7; Table S4). Serum cytokines were measured using the human Th1/Th2/Th17 cytometric bead array kit. Blood HCMV viral loads were quantified by DNA PCR (Supplemental Methods S.8).

S.7. Gene expression analysis for transplant subjects

Total RNA was extracted using QIAamp RNA Blood Mini Kit (Qiagen, Germantown, MD). First strand cDNA was synthesized from 200 ng of total RNA and a mixture of Oligo (dT) and random hexamer primers in a 20 µl reaction volume using RevertAid first strand cDNA synthesis Kit (Thermofisher Scientific, Waltham, MA). Purity of the cDNA was measured by A260/A280 ratio using UV spectroscopy (Thermofisher Scientific, Waltham, MA). Relative gene expression of RORγt and FOXP3 was performed using Real Time PCR (Lightcycler 480, Roche Molecular System, Pleasanton, CA), SYBR Green and primers specific to RORγt, FOXP3 and β-actin (Table S6) [7]. The amplification protocol consisted of 95°C for 10 minutes, followed by 45 cycles of 95°C for 10 seconds, 60°C for 15 seconds and 72°C for 20 seconds. Relative gene expression level (Fold Change) was calculated using the $2^{-\Delta\Delta C_T}$ method and the quantitation was normalized to endogenous gene expression of β- actin.

S.8. HCMV viral load quantitation

The HCMV viral load was performed using genomic DNA extracted from peripheral EDTA blood, as described previously.[8] Briefly, HCMV glycoprotein B gene (gB) in the DNA sample was amplified in Lightcycler 480 real time PCR platform (Roche Molecular System, Pleasanton, CA) using TaqMan probe (LightCycler TaqMan Master, Roche Molecular System, Pleasanton, CA) and primers specific to HCMV gB (Table S4).[8] The amplification protocol consisted of 95°C for

10 minutes, followed by 45 cycles of 58°C for 10 seconds and 72°C for 20 seconds. Viral copies/ml of peripheral blood was calculated using the standard curve generated with serially diluted cloned DNA standard plasmids (Roche Molecular System, Pleasanton, CA).
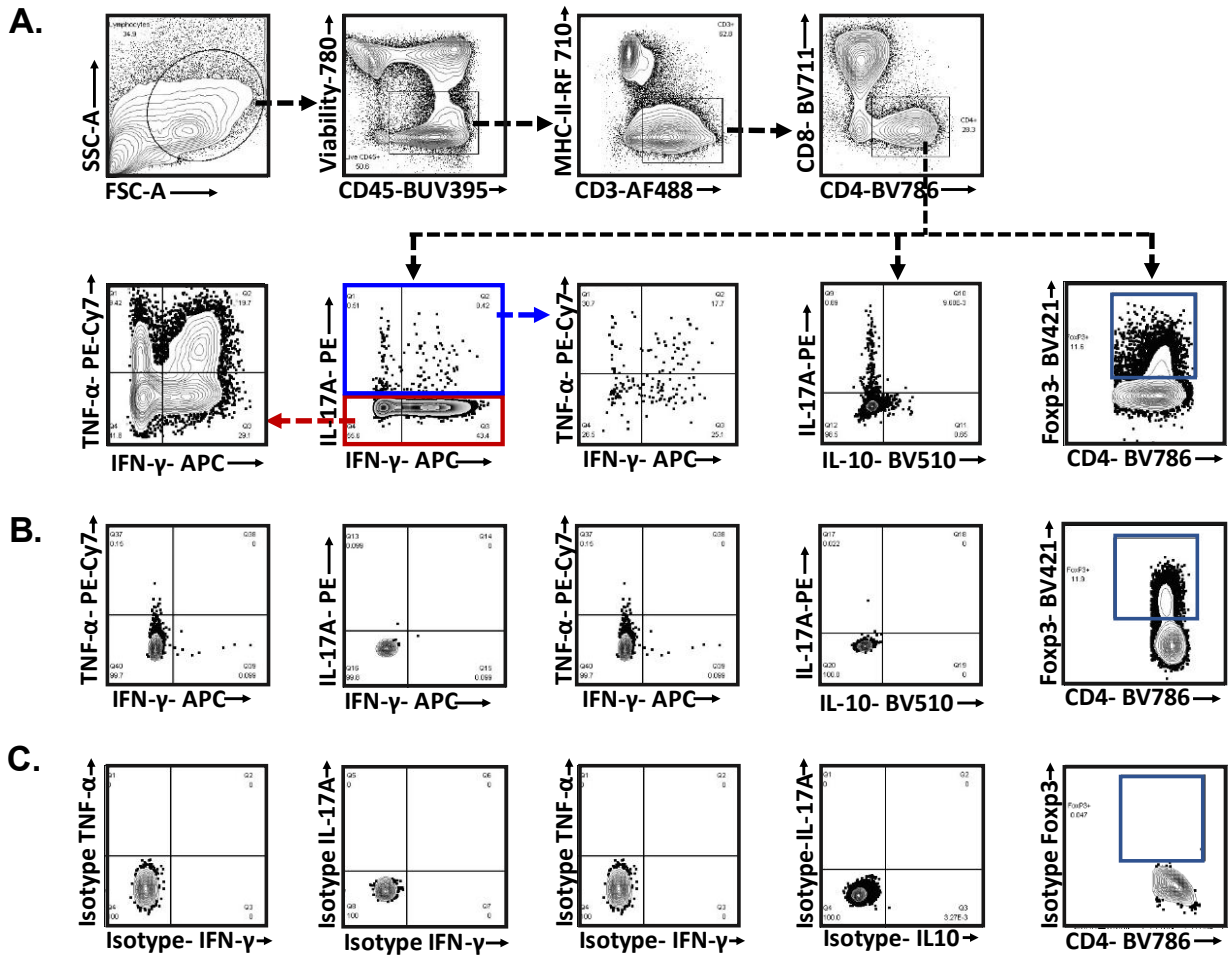
Figure S1. Flow cytometry gating strategy. (A) Gating strategy for cytokine expressing intragraft Th1, Th17, and Treg cells, shown after PMA/ionomycin stimulation. Lymphocytes were first identified by a forward scatter (FSC) and side scatter (SSC) gate. Viable CD45$^+$ cells were gated and CD4$^+$ T cells were identified within CD3$^+$MHCII$^-$ gate. Th17 cells were identified as IL-17A expressing CD4$^+$ T cells (blue square). IL-17A$^-$IFN-γ^+/TNF-α^+ CD4$^+$ T- cells were identified as Th1 cells (red square). FoxP3$^+$ CD4$^+$ T- cells were identified as Tregs. (B) Representative flowplots showing gating of cells incubated without PMA/ionomycin (no-stimulation condition). (C) Representative flowplots showing gating of cells after PMA/ionomycin stimulation, with isotype control staining for intracellular cytokines and Foxp3.
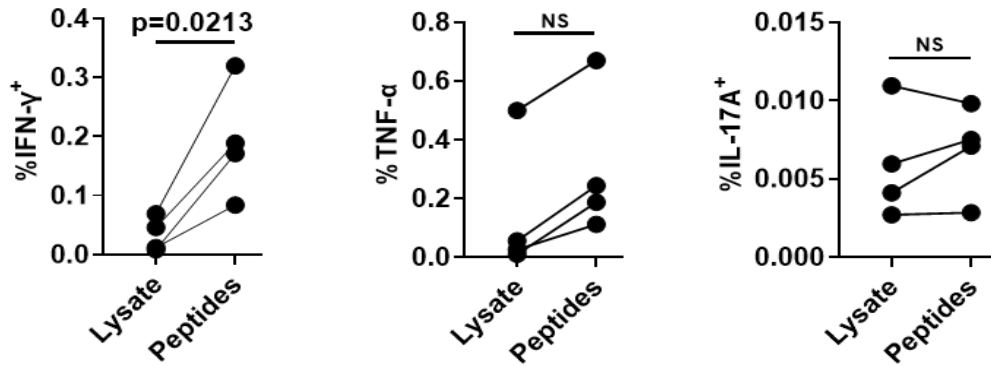
Figure S2. Comparison of MCMV-specific CD4^{+} T cell responses after stimulation with viral lysate or MCMV peptides. Splenocytes from D+R+ transplants were stimulated with MCMV lysate or a pool of 15 class II-restricted MCMV peptides (Table S3), stained for IFN-γ, TNF-α and IL-17A, and frequencies of CD4^{+} T cells expressing cytokines calculated after lysate or peptide stimulation. The differences between the two groups were analyzed using two- sided Student's t test. NS, not significant (p>0.05).
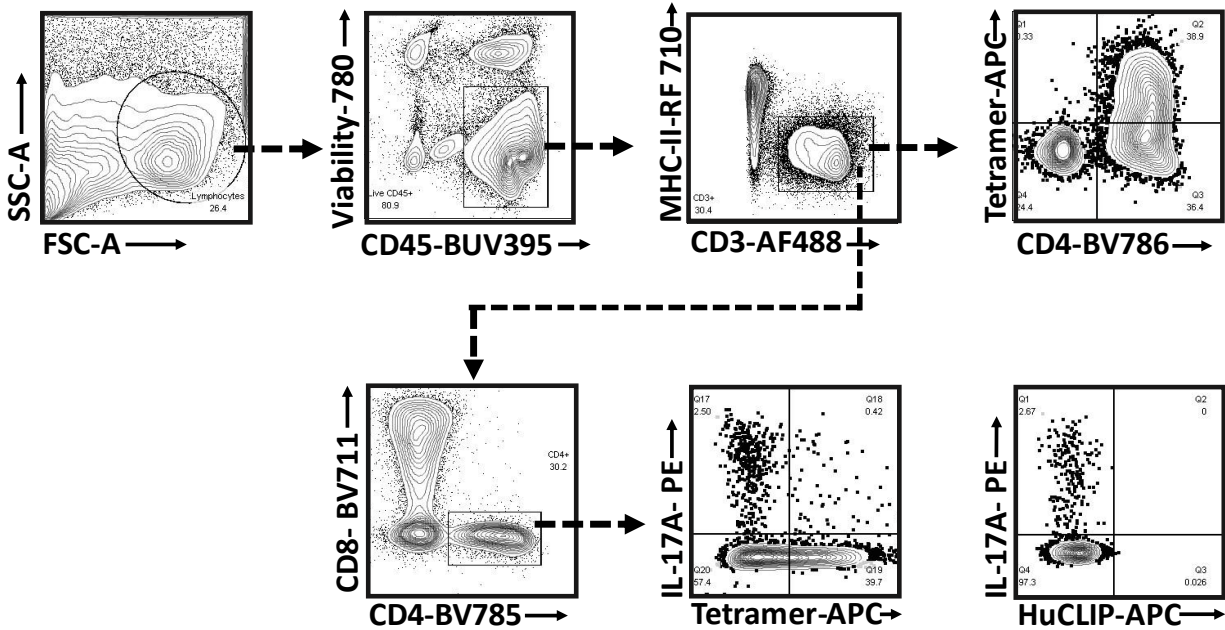
Figure S3. Flow cytometry gating strategy for I-A^b-OVA$_{323-339}$-APC tetramer$^+$ cells. CD3$^+$MHCII$^-$ T- cells were gated as described previously. I-A^b-OVA$_{323-339}$-APC tetramer$^+$ CD4$^+$ T- cells were identified within CD3$^+$MHCII$^-$ T- cells and IL-17A$^+$ OVA tetramer$^{+/-}$ cells were gated within CD4$^+$ T- cells. HuCLIP-APC tetramers were used as control staining for the OVA$_{323-339}$-APC tetramer. HuCLIP, Human MHC Class II-associated invariant chain.
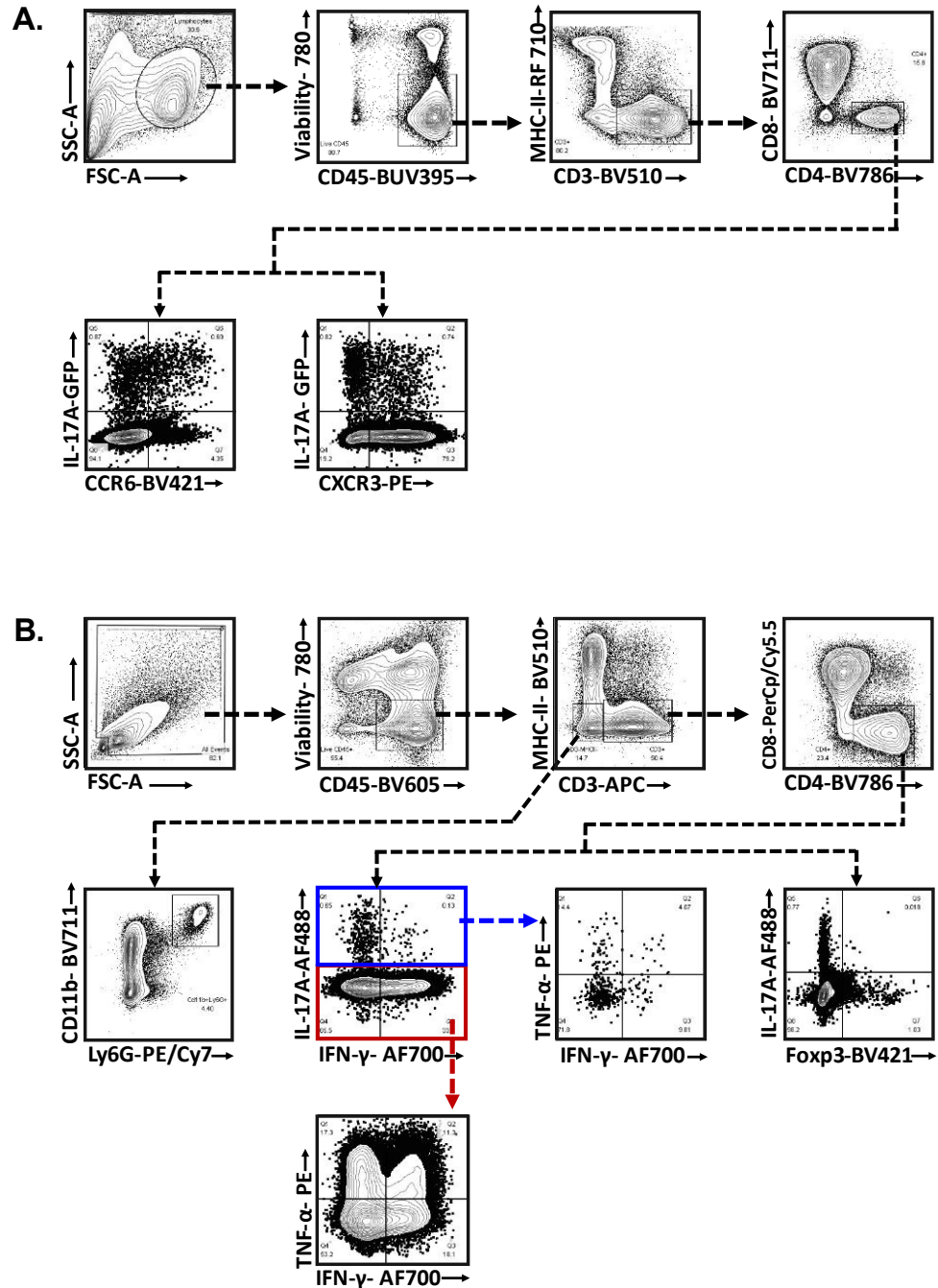
Figure S4. Flow cytometry gating strategy. (A) Expression of chemokine receptors by Th17 cells. CD4$^+$ T-cells were gated on live CD45$^+$MHCII$^-$CD3$^+$ T- cells as described previously. CCR6$^+$/CXCR3$^+$IL-17A$^+$ cells were identified within CD4$^+$ T- cells gate. (B) Neutrophil and cytokine expressing CD4$^+$ T- cells in anti- IL-17A and Isotype treated recipient mice. CD11b$^+$Ly6G$^+$ neutrophils were gated on live CD45$^+$MHCII$^-$CD3$^-$ populations. Th1, Th17 and Tregs were gated as described previously.
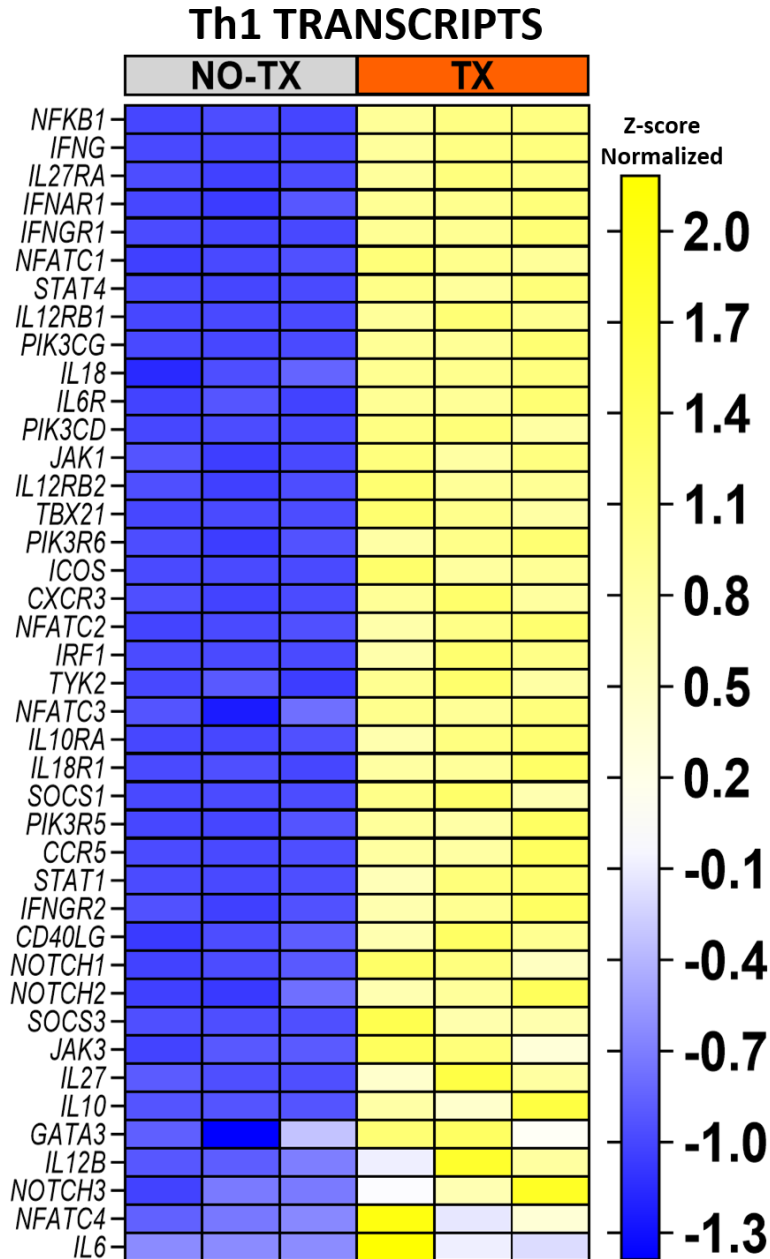
Figure S5. Differential expression of Th1 transcripts between D- allografts (TX) and native non-transplant MCMV uninfected kidneys (NO-TX). Differential expression of transcripts associated with Th1 cell differentiation and transcription factors. Hierarchical clustering of the genes was performed based on the average column z- score, highest to lowest.
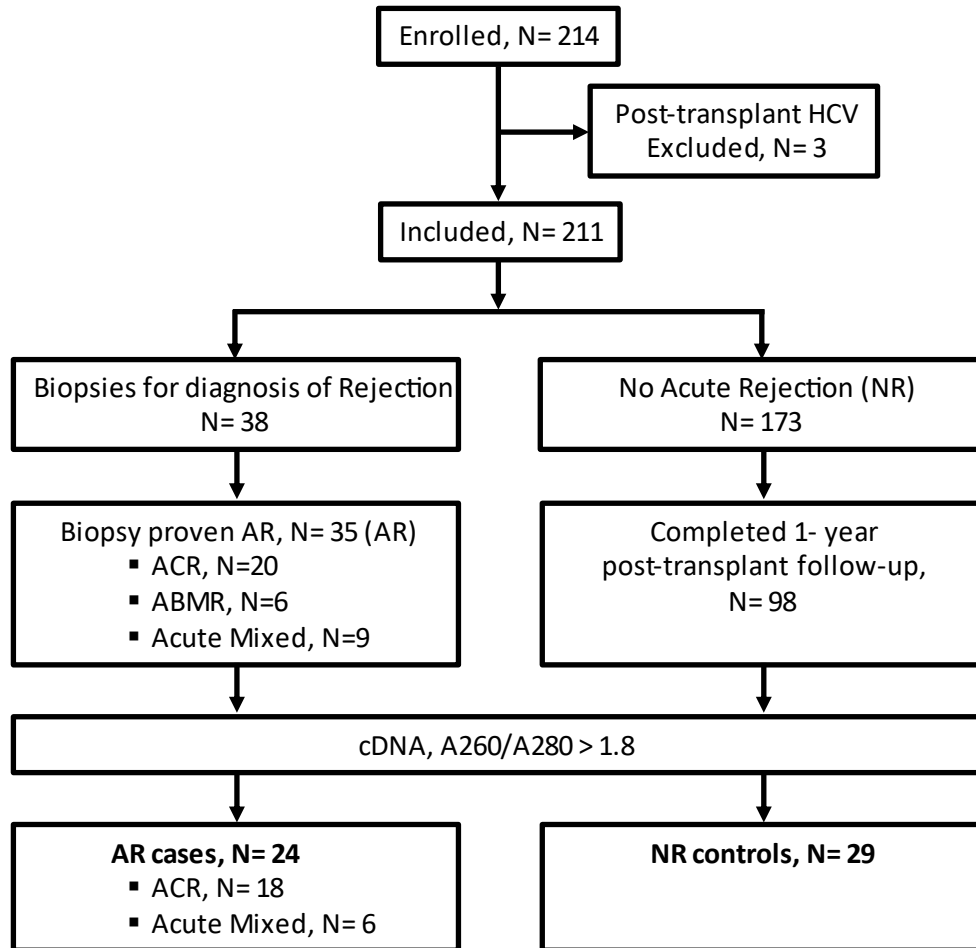
Figure S6. Study population. Of 214 enrolled patients, 3 were excluded due to post-transplant HCV infection. Of the 211 remaining patients, 35 had biopsy proven acute rejection (AR), of whom 24 patients had either ACR or acute mixed rejection and blood RNA samples of sufficient quality for RT-PCR analysis (AR group). Of the 173 patients without AR, 29 patients (NR group) with blood RNA of sufficient quality for RT-PCR were matched by age and sex to patients in the AR group. HCV, Hepatitis- C virus; cDNA, complementary DNA; AR, Acute Rejection.

Table S1. Class II restricted MCMV peptides[9]

Name	Locus	AA sequence	Mass (Da)	HCMV homologue
m09	133–147	GYLYIYPSAGNSFDL	1679.2	NA
m18	872–886	NERAKSPAAMTAEDE	1619.2	NA
M25	409–423	NHLYETPISATAMVI	1659.2	UL25
M45	102–116	AVSAANAAVNAAAAA	1242.3	UL45
M45	192–206	TPAATTPAATAVENR	1470.5	UL45
M45	239–253	QATPSTPIPIPAPRC	1548.1	UL45
M45	796–810	RPAVCGPGVSVVSGG	1341.3	UL45
M83	229–243	TLRYAKANGTPPDSL	1603.5	UL83 (pp65)
M104	261–275	LKRFIYAEPTILEEE	1851.3	UL104
M122/IE3	390–404	DRTAGGYVAPNAHKK	1584.6	UL122 (IE2)
m139	497–511	GSPWKTSAVTVSRKA	1574.2	US22
m139	560–574	TRPYRYPRVCDASLS	1784.4	US22
m141	181–195	LVVFSDPNADAATSV	1505.4	US24
m142	24–38	RSRYLTAAAVTAVLQ	1619.2	US26
m146	1–15	MTTPSPIRVRAIAVW	1698.5	NA

Abbreviations: AA, amino acid; HCMV, Da, Dalton; human cytomegalovirus; MCMV, murine cytomegalovirus; NA, not applicable (no known homologue)

Table S2. Flow Cytometry Panels

Laser	Marker	Flurophore	Clone ID	Dilution factor	Catalogue #
Th1/Th17/Tregs Panel					
355	Anti-CD45	BUV395	30-F11	BD Bioscience	565967
405	Anti-Foxp3	BV421	MF-14	Biolegend	126419
405	Anti-IL10	BV510	JES5-16E3	BD Bioscience	563277
405	Anti- CD8a	BV711	53-6.7	Biolegend	100747
405	Anti-CD4	BV785	GK 1.5	Biolegend	100453
488	Anti-CD3	AF488	17A2	Biolegend	100210
561	Anti-IL17A	PE	TC-11-18H10.1	Biolegend	506903
561	Anti-TNFα	PE/Cy7	MP6-XT22	Biolegend	506324
640	Anti-IFN-γ	APC	XMG1.2	Biolegend	505810
640	Anti-MHC-II (I-A/I-E)	RF710	M5/114.15.2	Tonbo Biosciences	80-5321-U100
640	Fixable Viability Stain 780	N/A	N/A	BD Bioscience	565388
Chemokine Receptor Panel					
355	Anti-CD45	BUV395	30-F11	BD Bioscience	565967
405	Anti-CCR6	BV421	29-2L17	Biolegend	129817
405	Anti-CD3	BV510	17A2	Biolegend	100233
405	Anti- CD8a	BV711	53-6.7	Biolegend	100747
405	Anti-CD4	BV785	GK 1.5	Biolegend	100453
488	IL-17A	Endogenous GFP Expression			
561	Anti-CXCR3	PE	CXCR3-173	Biolegend	126505
640	Anti-IFN-γ	APC	XMG1.2	Biolegend	505810
640	Anti-MHC-II (I-A/I-E)	RF710	M5/114.15.2	Tonbo Biosciences	80-5321-U100
640	Fixable Viability Stain 780	N/A	N/A	BD Bioscience	565388
Tetramer Staining Panel					
355	Anti-CD45	BUV395	30-F11	BD Bioscience	565967
405	Anti- CD8a	BV711	53-6.7	Biolegend	100747
405	Anti-CD4	BV785	GK 1.5	Biolegend	100453
488	Anti-CD3	AF488	17A2	Biolegend	100210
561	Anti-IL17A	PE	TC-11-18H10.1	Biolegend	506903
640	Tetramer	APC	N/A	NIH	N/A
640	Anti-MHC-II (I-A/I-E)	RF710	M5/114.15.2	Tonbo Biosciences	80-5321-U100
640	Fixable Viability Stain 780	N/A	N/A	BD Bioscience	565388
Neutrophil Panel					
405	Anti-Foxp3	BV421	MF-14	Biolegend	126419
405	Anti-MHC-II (I-A/I-E)	BV510	M5/114.15.2	Biolegend	107635
405	Anti-CD45	BV605	30-F11	Biolegend	103140
405	Anti-CD11b	BV711	M1/70	Biolegend	101241
405	Anti-CD4	BV785	GK 1.5	Biolegend	100453
488	IL-17A	AF488	TC11-18H10	BD Bioscience	560220
488	Anti-CD8	PerCP/Cy5.5	53-6.7	Biolegend	100733
561	Anti-TNFα	PE	MP6-XT22	BD Bioscience	561063
561	Anti-Ly6G	PE/Cy7	1A8	Biolegend	127617
640	Anti-CD3	APC	17A2	Biolegend	100236
640	Anti-IFN-γ	AF700	XMG1.2	Biolegend	505824
640	Fixable Viability Stain 780	N/A	N/A	BD Bioscience	565388

Table S3. Murine Histology Scoring Criteria (based on clinical criteria)[10,11]

Inflammation; avoid fibrotic areas, subcapsular cortex, and lymphatics
0 = <10% of unscarred cortical parenchyma
1 = 10 to 25% of unscarred cortical parenchyma
2 = 26 to 50% of unscarred cortical parenchyma
3 = >50% of unscarred cortical parenchyma
add asterisk if there are 5 to 10% eosinophils, neutrophils or PCs

Tubulitis; cut longitudinally; number of mononuclear cells per 10 TEC; most severely affected tubule determines score; avoid atrophic tubules (<25% of normal tubular diameter)
0 = No mononuclear cells or a single focus
1 = Foci with 1 to 4 mononuclear cells / tubular cross section
2= Foci with 5 to 10 mononuclear cells / tubular cross section
3= Foci with >10 mononuclear cells / tubular cross section or presence of ≥ areas of TBM destruction accompanied by i2 to i3 scores elsewhere

Arteritis; more than 2 sm mm cell layers; WBCs in subendothelial space; most severe dictates score; arterioles do not count; mural inflammation does not count; asterisk if there is TI hemorrhage and or infarcts
0 = No arteritis
1= Mild to moderate in at least 2 arteries
2= Severe with at least 25% of the luminal area lost in at least 1 artery
3= Transmural arteritis and / or fibrinoid change and sm mm cell necrosis with Lcic infiltrate in the vessel

Glomerulitis; both endothelial and WBCs must contribute to the occlusion of the glomerular capillary lumen; denominator is number of non-sclerotic gloms
0 = No glomerulitis
1= segmental to global glomerulitis in <25% of gloms
2= segmental to global glomerulitis in 25 to 75% of gloms
3 = segmental to global glomerulitis in >75% of gloms

PTC; only cortex; use asterisk if to indicate only mononuclear cells and no nfls; use focal or diffuse but that does not contribute to score; avoid pyelo, necrotic regions and inflamed subcapsular cortex; only cross section PTCs
0= Maximum number of leukocytes <3
1= at least 1 leukocyte in ≥ 10% of cortical PTCs with only 3 to 4 WBCs in the most severely involved PTC
2= at least 1 leukocyte in ≥ 10% of cortical PTCs with only 5 to 10 WBCs in the most severely involved PTC
3 = at least 1 leukocyte in ≥ 10% of cortical PTCs with >10 WBCs in the most severely involved PTC

Cortical interstitial fibrosis:
0= Interstitial fibrosis in up to 5% of cortex
1 = Interstitial fibrosis in up to 6 to 25% of cortex
2= Interstitial fibrosis in up to26 to 50% of cortex
3 = Interstitial fibrosis in > 50% of cortex

Cortical tubular atrophy; tubules with a thickened TBM or a decrease diameter of lumen >50%

0 = No tubular atrophy

1= Tubular atrophy >25% of the area of the cortical tubules

2= Tubular atrophy involving 26 to 50% of the area of the cortical tubules

3= Tubular atrophy involving >50% of the area of the cortical tubules

---

Vascular fibrous intimal thickening; assess most severely affected artery; does not discriminate b/t bland fibrosis and fibrosis containing WBCs

0= No chronic vascular changes

1= Vascular narrowing up to 25% of luminal area

2= Vascular narrowing up to 26 to 50% of luminal area

3 = Vascular narrowing >50% of luminal area

Mesangial matrix expansion; non sclerotic gloms

0= No more than mild mesangial matrix increase in any glomerulus

1= expansion of matrix to exceed the width of 2 mesangial cells in at least 2 lobules in up to 25% of gloms

2= expansion of matrix to exceed the width of 2 mesangial cells in at least 2 lobules in 26 to 50% of gloms

3= expansion of matrix to exceed the width of 2 mesangial cells in at least 2 lobules in > 50% of gloms

---

Arteriolar hyalinosis; nodular hyaline in arterioles; add asterisk of arteriolaritis is also present

0 = not present

1= Mild to moderate in at least 1 arteriole

2 = moderate to severe in more than 1 arteriole

3= severe in many arterioles

Total inflammation; extent of cortical inflammation includes areas of IFTA, subcapsular cortex and perivascular regions

0 = no or trivial inflammation (<10% of total cortex)

1= 10-25% of cortical parenchyma is inflamed

2= 26-50% of cortical parenchyma is inflamed

3 = >50% of cortical parenchyma is inflamed

IFTA; inflammation in scarred regions

0 = no or trivial inflammation (<10% of total cortex)

1= 10-25% of scarred cortical parenchyma is inflamed

2= 26-50% of scarred cortical parenchyma is inflamed

3 = >50% of scarred cortical parenchyma is inflamed

Table S4. Primer sequences

Primers	Sequence
FOXP3 and RORγt[7]	
β-actin Forward	5'- GAGCTACGAGCTGCCTGACG - 3'
β- actin Reverse	5'- GTAGTTTCGTGGATGCCACAG- 3'
RORγt Forward	5'- GCTACCCTACTGAGGAGGACAG- 3'
RORγt Reverse	5'- ATTACACTGCTGGCTGCGGCGGAAG-3'
FOXP3 Forward	5'- GAAACAGCACATTCCAGAGTTC- 3'
FOXP3 Reverse	5'- ATGGCCCAGCGGATGAG- 3'
HCMV glycoprotein B (gB)[8]	
HCMV gB Forward	5'- GCACCATCCTCCTCTTCCT- 3'
HCMV gB Reverse	5'- GGCCTCTGATAACCAAGCC- 3'
MCMV Immediate Early (IE1) exon 4[8]	
MCMV IE1 Forward	5'-ACATCTTTGAGCGTGACTACC-3'
MCMV IE1 Reverse	5'- GTGCCGTTCACCGTAGAATTA-3'

Table S5. Top 20 Canonical Pathways

CANONICAL PATHWAYS	Negative log (p-value)		Number of genes Counted	
	CMV+ NON-TX KIDNEYS	D+R+ ALLOGRAFTS	CMV+ NON-TX KIDNEYS	D+R+ ALLOGRAFTS
Systemic Lupus Erythematosus In B Cell Signaling Pathway	21.08164972	25.95900033	118	131
Th1 and Th2 Activation Pathway	**13.75590187**	**22.53811369**	**74**	**91**
Hepatic Fibrosis / Hepatic Stellate Cell Activation	21.70088729	22.2423348	94	98
Coronavirus Pathogenesis Pathway	20.56129928	19.79231696	95	97
Molecular Mechanisms of Cancer	20.94039557	19.36791713	164	167
Role of Macrophages, Fibroblasts and Endothelial Cells in Rheumatoid Arthritis	15.55768639	17.84955671	120	130
TREM1 Signaling	13.83847422	17.80059948	44	50
Granulocyte Adhesion and Diapedesis	8.581582994	17.11898893	68	88
Role of Pattern Recognition Receptors in Recognition of Bacteria and Viruses	10.38413486	16.87887055	63	77
Hepatic Fibrosis Signaling Pathway	16.61316064	16.53592171	147	153
Colorectal Cancer Metastasis Signaling	15.12491939	16.01942981	104	110
Th1 Pathway	10.81494641	15.82139995	54	64
Tumor Microenvironment Pathway	11.1690174	14.92668084	71	81
Natural Killer Cell Signaling	14.92590679	14.86409015	84	87
Kinetochore Metaphase Signaling Pathway	14.8626083	14.34633014	55	56
Signaling by Rho Family GTPases	14.32051505	13.39677906	102	104
Breast Cancer Regulation by Stathmin1	10.56473732	13.14502451	171	188
Cardiac Hypertrophy Signaling (Enhanced)	10.40370375	12.98693223	158	174
Phagosome Formation	11.41643415	12.86868355	63	68
PI3K/AKT Signaling	12.86126645	12.82619018	80	83

Table S6. Renal Transplant Patient Demographics

Variables	No rejection (NR), N= 29	Acute Rejection (AR), N=24
Median Age in Years (Range)	40 (20- 58)	34 (12-44)
Gender		
Male	24 (82.75%)	20 (83.34%)
Female	5 (17.24%)	4 (16.66%)
Underlying disease for ESRD		
CGN-CRF	14 (48.27%)	9 (37.50 %)
Hypertension	7 (24.13%)	9 (37.50 %)
Diabetic Nephropathy	3 (10.34%)	1 (4.16%)
IgA Nephropathy	1 (3.44%)	2 (8.33%)
Other[a]	3 (10.34%)	3 (12.50%)
Allograft Donor		
Living related	13 (44.80%)	14 (58.33%)
Living Unrelated	11 (37.93%)	6 (25.00%)
Deceased	5 (17.24%)	4 (16.66%)
HLA Mismatch	4.0 ± 1.9 (0- 6)	4.0 ± 1.4 (2- 6)
Induction Immunosuppression		
ATG	1 (3.44%)	1 (4.16 %)
Anti IL2R	4 (13.79%)	5 (20.83%)
None	24 (82.75%)	18 (75.00%)
Maintenance Immunosuppression		
Tac/MMF/Steroid	27 (93.10%)	24 (100%)
CsA/MMF/ Steroid	1 (3.44%)	0
Tac/AZA/Steroid	1 (3.44%)	0
Acute Rejection Type		
ACR	NA	18 (75.00%)
Mixed	NA	6 (25.00%)
Mean onset of Rejection, days	NA	32.44 ± 49.46

[a]Alport syndrome; autosomal dominant polycystic kidney disease; collapsing thrombotic microangiopathy; obstructive uropathy.

Abbreviations: ACR, Acute cellular rejection; ATG, Anti-thymocyte globulin; AZA, Azathioprine; CGN-CRF, Chronic Glomerulonephritis-Chronic renal failure; CsA, Cyclosporine A; ESRD, End-stage renal disease; HLA, Human leukocyte antigen; MMF, Mycophenolate Mofetil; Tac, Tacrolimus.

Table S7. HCMV DNAemia in NR and AR groups.

DNAemia Group	NR	AR	P value*
CMV-	16	12	
CMV+	1	8	0.0159
Total	17	20	

*Chi-square test.

Abbreviations: AR, Acute Rejection; CMV, Cytomegalovirus; NR, No Rejection.

Supplemental References

1.   Dobin A, Davis CA, Schlesinger F, et al. Star: Ultrafast universal rna-seq aligner. *Bioinformatics.* 2013;29(1):15-21. doi: 10.1093/bioinformatics/bts635.
2.   Love MI, Huber W, Anders S. Moderated estimation of fold change and dispersion for rna-seq data with deseq2. *Genome Biol.* 2014;15(12):550. doi: 10.1186/s13059-014-0550-8.
3.   Li M, Boddeda SR, Chen B, et al. Nk cell and th17 responses are differentially induced in murine cytomegalovirus infected renal allografts and vary according to recipient virus dose and strain. *Am J Transplant.* 2018;18(11):2647-2662. doi: 10.1111/ajt.14868.
4.   Dhital R, Minz M, Minz RW, et al. Flow cytometric quantitation of t-cell subsets in peripheral blood of renal allograft recipients. *Indian Journal of Transplantation.* 2016;10(4). doi: 10.1016/j.ijt.2016.09.031.
5.   Dhital R, Minz M, Minz RW, et al. Or19 quantification of peripheral b-cell subsets in acute allograft rejection in recipients with renal transplantation. *Human Immunology.* 2016;77. doi: 10.1016/j.humimm.2016.07.031.
6.   Minz M, Dhital, R., Jha, V., Minz, R.W., Sharma, A. Mrna expression of baff and april receptors increases in acute rejection in kidney transplant recipients. *Am J Transplant.* 2016;16.
7.   Mitra S, Anand S, Das A, Thapa B, Chawla YK, Minz RW. A molecular marker of disease activity in autoimmune liver diseases with histopathological correlation; foxp3/rorgammat ratio. *APMIS.* 2015;123(11):935-944. doi: 10.1111/apm.12457.
8.   Minz RW, Kumar M, Kanwar DB, et al. Cytomegalovirus infection in postrenal transplant recipients: 18 years' experience from a tertiary referral center. *Transplant Proc.* 2020;52(10):3173-3178. doi: 10.1016/j.transproceed.2020.02.162.
9.   Arens R, Wang P, Sidney J, et al. Cutting edge: Murine cytomegalovirus induces a polyfunctional cd4 t cell response. *J Immunol.* 2008;180(10):6472-6476. doi: 10.4049/jimmunol.180.10.6472.
10.   Loupy A, Haas M, Roufosse C, et al. The banff 2019 kidney meeting report (i): Updates on and clarification of criteria for t cell- and antibody-mediated rejection. *Am J Transplant.* 2020;20(9):2318-2331. doi: 10.1111/ajt.15898.
11.   Roufosse C, Simmonds N, Clahsen-van Groningen M, et al. A 2018 reference guide to the banff classification of renal allograft pathology. *Transplantation.* 2018;102(11):1795-1814. doi: 10.1097/TP.0000000000002366.